Scripta Materialia **65 (2011) 288–291**

Extreme anelastic responses in $Zn_{80}Al_{20}$ matrix composite materials containing $BaTiO_3$ inclusion

Liang Dong,[a] Donald S. Stone,[b] and Roderic S. Lakes[a,b,c]
[a]*Department of Engineering Physics, University of Wisconsin, Madison, WI 53706-1687, USA*
[b]*Materials Science Program, University of Wisconsin, Madison, WI 53706-1687, USA*
[c]*Engineering Mechanics Program, University of Wisconsin, Madison, WI 53706-1687, USA*

Abstract: Extreme anelastic responses (stiffness greater than diamond and large amplification of damping) due to the presence of a negative stiffness phase have been observed in $Zn_{80}Al_{20}$-$BaTiO_3$ composites not only near the tetragonal-orthorhombic transformation temperatures of $BaTiO_3$ anticipated by the classical Landau theory, but far below the Curie point of $BaTiO_3$ which can be manipulated via specific aging processes that operated by an oxygen vacancy mechanism. The idea proposed herein can be utilized to fabricate novel composites for potential engineering applications.

***Keywords*:** metal matrix composite, anelastic behavior, negative stiffness, ferroelastic materials

Composite properties, such as stiffness, damping, thermal expansion, piezoelectricity, etc., cannot surpass those of the constituents according to the classical composite theory. However, such bounds can be exceeded if the composite has a negative stiffness phase.[1] Negative stiffness entails a reversal of the usual directional relationship between force and displacement in deformed objects. Negative stiffness can be entailed in lumped systems, such as buckled tubes [1], and ferroelastic materials, such as VO_2 and $BaTiO_3$, during phase transformations according to the classical Landau theory. The concept of making advanced composites by incorporating negative stiffness phase has been known since 2001[1], and impressively demonstrated in real materials such as Sn-VO_2 [2] and Sn-$BaTiO_3$ [3] in subsequent years. In particular, a viscoelastic stiffness greater than that of diamond has been observed in Sn-$BaTiO_3$ [3] composites over a narrow range of temperature where a negative stiffness effect of the inclusion is entailed. Surprisingly, the extreme composite responses occurred near 60°C, far below the Curie point (*Tc*~130°C) of $BaTiO_3$; only a small sigmoid anomaly was observed near 130°C [3]. Such a phenomenon cannot be explained via known transformations of $BaTiO_3$ as the classical Landau theory predicts a negative bulk stiffness in constrained $BaTiO_3$ only near its three first order ferroelastic transformation temperatures (130°C: cubic-to-tetragonal, 5°C: tetragonal-to-orthorhombic, and -75°C: orthorhombic-to-rhombohedral. Stress induced temperature shift is minimal because Sn will yield at 30MPa [4] which can merely lower [5] *Tc* and tetragonal-orthorhombic transition temperature of $BaTiO_3$ by less than 2°C). Also, such intense responses were not able to survive over multiple thermal cycles in Sn-$BaTiO_3$, a fact largely due to a weak interfacial strength.

In this work, the anelastic properties of $Zn_{80}Al_{20}$-$BaTiO_3$ composites have been studied. In particular, ferroelectric-aging-process-activated extreme composite responses (including stiffness greater than diamond) have been observed far below *Tc* (the same temperature region for the extreme responses observed in Sn-$BaTiO_3$ [3]). Anomalies persisted over multiple thermal cycles through *Tc*. Such an extreme composite responses entailed via ferroelectric aging can be eliminated via paraelectric aging. In view of its aging process dependence, we explained such phenomena in the context of an oxygen vacancy mechanism [6] caused negative stiffness effect in $BaTiO_3$. To the best of our knowledge, this is the first experimental report of a manipulation (activation and deactivation) of negative stiffness in ferroelastic inclusion via specific aging processes to attain extreme composite responses, an advance in the field of composite materials with negative stiffness phase. As impurities are inevitable species in ferroelectric materials, which must be compensated by oxygen vacancies to keep electric neutrality, the concept proposed herein to induce negative stiffness in ferroelastic materials via the defect mechanism is of significant importance and generic interest for various applications where actuation tunable negative stiffness effect is required. Extreme responses (large amplification of damping and stiffness greater than diamond) anticipated by the classical Landau theory have also been found near the tetragonal-orthorhombic transition zone of $BaTiO_3$. Near *Tc*, a modest increase in modulus and damping was observed. Explanation has been given for such a response difference near the normal ferroelastic transformations, which has a generic implication for the appropriate choice of ferroelastic materials as negative stiffness phase for attaining intended composite responses operated by normal ferroelastic transformations.

$Zn_{80}Al_{20}$ matrix composites (with ~5% volume inclusions) were fabricated via an ultrasonic casting technique [7] using 150-210μm particulate polycrystalline $BaTiO_3$ (Alfa Aesar, 99.9%; 25μm average grain size, 1μm smallest domain size). $Zn_{80}Al_{20}$ was selected as the matrix for its strength greater than that of tin to minimize separation between inclusions and matrix at the interface; also to minimize the segregation problem of the inclusion during casting as it has similar density as $BaTiO_3$ (5.85×10^3g/cm^3). ZnAl alloys are used in industry; their properties provide a meaningful baseline. Mixture (4:1 weight ratio) of Zn shots (Alfa Aesar, 99.99%) and Al shots (Alfa Aesar, 99.9%) was first superheated to 700°C, stirred with an Al_2O_3 rod for complete mixing. The molten matrix alloy was then cooled gradually to 500°C, and dispersion of preheated (500°C) $BaTiO_3$ particles in the matrix melt was achieved by means of ultrasonic waves emitted from the end of a titanium coupler rod placed well below the melt surface. Sonication was performed at about 500°C for 10 min under argon protection. Pure $Zn_{80}Al_{20}$ was processed with the same procedures to obtain similar microstructure as the composite matrix. $Zn_{80}Al_{20}$–SiC (with ~5% volume 150-210μm particulate inclusions) has also been synthesized for comparison. Specimens of typical size $1.8\times2\times20$ mm^3 were sectioned with a low speed abrasive diamond saw, and were then annealed at 190°C (~0.4*Tm*) in air under atmospheric pressure for 5h to release internal stress. The anelastic properties (damping and Young's modulus) of the specimens were studied in bending at subresonant frequencies (bending resonant frequency is about 1300Hz) with broadband viscoelastic spectroscopy [8]. Sufficient aging (in air at atmospheric pressure) was performed *in situ* at either below or above *Tc* prior to testing. Sufficient aging does not necessarily mean complete aging. Sufficient aging below (or above) *Tc* can be performed at any temperature in the tetragonal (or cubic) $BaTiO_3$ and will not affect the responses [6]. Maximum surface strain applied was about 8×10^{-6}. A thermal rate between 0.04 and 0.06°C/s was used. Temperature was monitored by a thermocouple directly in contact with specimen surface.

Figure 1(a) and (b) show the extreme anelastic responses (Young's modulus $|E^*|$ and damping $\tan\delta$) of a composite specimen (I) in a consecutive first **(a)** and second **(b)** heating scans after ferroelectric aging (i.e. aging below *Tc*) at 55°C for 20h. The stiffness of this specimen has surpassed that of diamond (**Figure 1a**) over a narrow range of temperature far below *Tc*. Extreme responses sustained for at least four thermal scans passing through *Tc* (further thermal scans were not performed). Responses became weaker with thermal scans, a phenomenon attributed to the neutralization effect of aging above *Tc*. Such extensive composite responses were not observed after subjecting the specimen to paraelectric aging (i.e. aging above *Tc*) at 185°C for 4h (as shown in **Figure 1b** also **Figure 1c**). No anomaly was seen in $Zn_{80}Al_{20}$ matrix or in $Zn_{80}Al_{20}$-SiC after 55°C 20h aging as shown in (c). It should be noted here that the measurement after 185°C aging was conducted prior to the measurements after 55°C aging, hence extreme responses observed after ferroelectric aging were not due to residual stress introduced during sample preparation, and the disappearance of these extreme responses after paraelectric aging was not attributed to the interface failure after multiple thermal cycles through *Tc*. Subsequent paraelectric aging still eliminated the 55°C aging induced extreme responses. The baseline damping for the composite aged at 185°C was ~0.007 at 40°C to ~0.016 at 100°C. The composite aged at 55°C exhibited excursions in damping from -0.8 to +0.12 in the region between 50°C and 70°C. Negative damping is associated with release of stored energy; positive damping represents energy dissipation. The sharp spikes in the response are not noise because response of a similar size specimen of matrix alloy is smooth as shown (**Figure 1c**). The sharp responses cannot be due to relaxation mechanisms because they entail relatively broad humps in temperature or frequency dependence [9]; in particular, a relaxation process in tetragonal $BaTiO_3$ will give rise to a single broad peak spanning about 80°C wide in temperature [10]. Near *Tc*, moderate excursion about 15GPa (18%) in modulus with respect to baseline values was observed.

Tetragonal $BaTiO_3$ has a baseline stiffness (~100GPa) comparable to that of $Zn_{80}Al_{20}$ (~74GPa). The small 5% volume concentration of such inclusions is predicted to have a minimal stiffening effect according to this baseline modulus. Even if the inclusions were infinitely stiff, 5% by volume of such particles will increase the composite stiffness by only 11% (Hashin-Shtrikman bounds). The baseline stiffness of $Zn_{80}Al_{20}$-$BaTiO_3$ composite is about 80GPa (**Figure 1c**), an increase by ~8% compared with $Zn_{80}Al_{20}$. Such an overall stiffening effect has also been observed in $Zn_{80}Al_{20}$–SiC (**Figure 1c**) and ZA-27 (eutectic composition) matrix composites reinforced by hard inert inclusions (TiO_2, zircon) [11, 12], and is attributed to the high dislocation density in the matrix near the interface introduced during solidification as the constituents have very different thermal expansion coefficients. However, dislocation cannot explain the extreme anelastic responses observed in the ferroelectric-aged $Zn_{80}Al_{20}$-$BaTiO_3$ as no anomaly was observed in $Zn_{80}Al_{20}$-SiC after the same aging process (**Figure 1c**). The dramatic enhancement of composite stiffness and damping are attributed to the negative stiffness of the $BaTiO_3$ inclusions following analysis by composite theory [1]. Broadening effect is due to negative stiffness heterogeneity of local environment; this comes from the variation in the size, morphology, internal structure, defect concentration and surface constraint of individual inclusion particles.

Negative stiffness can occur in systems with stored elastic energy [1], including, via Landau theory, ferroelastic materials that undergo phase transformations under constraint. Negative stiffness has been predicted via molecular simulations to appear naturally on the nanoscale [13]. In our earlier work [14], we also found in well aged tetragonal $BaTiO_3$, negative stiffness can be entailed via electromagnetic interaction of defect polarization and spontaneous polarization. In view of the aging process dependence, the anomaly observed in the present $Zn_{80}Al_{20}$-$BaTiO_3$ composite specimens far below 130°C is considered to be associated with this defect mechanism. Such a process is understood in the context of symmetry-conforming property of point defects (SCP-PD) [6]. The oxygen octahedron in tetragonal $BaTiO_3$ is shown in Figure 3(a). O^{2-} has two kinds of nonequivalent sites: *A* (or *B*) and *C*. In the cubic phase, distances from *A*(*B*) and *C* sites to Ti^{4+} are the same; in the tetragonal phase, *C* sites are closer to Ti^{4+} than *A*(*B*) sites (bond lengths in the diagram are based on ref. [10]). Oxygen vacancy (OV) can occupy either of *A* (or *B*) sites or *C* sites of the oxygen octahedron (**Figure 2a**) with identical conditional probabilities above *Tc* as these sites have identical distances to the center of the octahedron. Below *Tc*, OV will migrate to and accumulate at *C* sites, which are closer to the center of octahedron, from *A*(*B*) sites during aging. As a result, defect polarization ($\mathbf{P_d}$), formed by impurities (such as Ti^{3+}, Al^{3+}) [15] located at Ti^{4+} site and OV, will appear after sufficient aging below *Tc*, which will generate a restoring stress on the spontaneous polarization ($\mathbf{P_s}$) [6]. By contrast, sufficient aging above *Tc* eliminates $\mathbf{P_d}$. **Figure 2b** (after [6]) presents a pertinent scheme showing the change of crystal and defect symmetries (in two dimensions for simplicity's sake) and the conditional probabilities of OV occupation among different conditions. P_i^{OV} (P_i^{A}) is the conditional probability of OV (or an atom *A*) occupying ion site *i* (1 and 2 correspond to *A* or *B* sites of oxygen octahedron; 3 and 4 correspond to *C* site of oxygen octahedron) when a defect "D" (such as Ti^{3+}, Al^{3+}) is occupying Ti^{4+} site (i.e., "0" site), and is represented by the area of the half circle shown in **Figure 2b**. **Figure 2c** shows the schematic of $\mathbf{P_s}$ and $\mathbf{P_d}$ below *Tc* after "ferroelectric aging" and "paraelectric aging". $\mathbf{P_s}$ (exists below *Tc* but not above) can change direction and magnitude under external stress (or lattice reconstruction in the case of ferroelastic transformation) instantaneously but not $\mathbf{P_d}$, the changing of which requires time (i.e. aging) for the rearrangement of atoms and OVs within the same sublattice [6]. Angular deviation between $\mathbf{P_s}$ and $\mathbf{P_d}$ will thus occur, causing stored elastic energy and a metastable condition for the system (**Figure 2d**). Snap-through is entailed under perturbations (external stress or nonlinear interaction between polarizations) which could transform the system towards a stable condition, and a negative stiffness effect is shown during this process. Specifically, in the potential well diagram at the right in **Figure 2d**, a perturbation causes a ball to slide down towards the bottom of the potential wells, giving rise to a negative stiffness effect. Interaction energy (*W*) between $\mathbf{P_s}$ and $\mathbf{P_d}$, and the elastic energy (*U*) are expressed as $W=(\mu_{\text{defect}}\,\mu_{\text{spontaneous}})/4\pi\varepsilon_0 r^3$[16] and $U=0.5E\varepsilon^2V$, respectively. Assuming $\mu_{\text{defect}} \approx \mu_{\text{spontaneous}} = 1.5\times10^{-29}$ C m ($\mathbf{P_s} = 24\times10^{-6}$C/cm^2) [17] within unit cell volume, the shortest interaction distance between $\mathbf{P_s}$ and $\mathbf{P_d}$ to induce negative stiffness (i.e. U and W are comparable) is several unit cell edge length as the local strain will be several orders (ultimate strain for tetragonal $BaTiO_3$ is about 1.8×10^{-3} [18]) of magnitude larger than the applied strain (8×10^{-6}) when localized negative stiffness is entailed [19].

Landau theory predicts a negative stiffness near the ferroelastic transformations in constrained $BaTiO_3$. Indeed, we have observed extremely high values of composite modulus and damping (composite specimen II) near the tetragonal-orthorhombic transformation zones (~25°C in heating and ~5°C in cooling) of $BaTiO_3$ inclusions (**Figure 3**). This specimen was pre-aged at 75°C for 18h, freely cooled to 0°C, then the heating scan (a) was conducted, then the cooling scan (b). Spontaneous strain involved during this transformation is about 4×10^{-5} [20], much smaller than 2×10^{-4} [20] near *Tc*. Results show the expected hysteresis in that the response temperature differs in heating and cooling. The modulus curve in cooling exhibits a peak greater than that of diamond; the sigmoid shape of the curve is as expected from the theory [1]. The damping exhibits a giant peak as well as a region of negative damping: large excursions by a factor of -17 to +99 (in cooling) in $\tan\delta$ occur from -0.1 to +0.6 with respect to baseline damping ~0.006 of $Zn_{80}Al_{20}$ near 5°C. Modulus is substantially elevated above baseline over a range of 8°C; damping is elevated over a range of about 12°C. The expansion of the range of temperature is attributed to a better balance of positive and negative stiffness for this transformation compared with ones studied previously [2, 3]. By contrast, $Zn_{80}Al_{20}$ matrix (after 75°C 18h aging) exhibited no anomaly.

Small undulations were observed rather than extreme responses near 130°C (*Tc* of $BaTiO_3$) in Sn-$BaTiO_3$ [3] and in the specimens tested in the present study. Landau theory predicts negative stiffness for each of the three ferroelastic transformations of $BaTiO_3$. The difference may be due to an insufficient constraint from the matrix for $BaTiO_3$ near *Tc* in view of the larger spontaneous strain (~2×10^{-4}) [20], and hence an insufficient negative stiffness value. Constraint by the matrix is necessary to prevent the negative stiffness effect from causing instability. The magnification of applied strain near the inclusion near *Tc* might overload the interface.

By contrast to the substantial spontaneous strain near *Tc*, the negative stiffness induced by an OV mechanism involves barely detectable macroscopic spontaneous strain (no more than 10^{-6}) [14] as the interaction between $\mathbf{P_s}$ and $\mathbf{P_d}$ occurs locally inside. The interface is less likely to be overloaded during such a process. Interface strength and matrix strength are essential to the performance of these composites. In that vein, the present $Zn_{80}Al_{20}$ (of strength~170MPa [4]; 2×10^{-4} strain induces stress ~15MPa) matrix composite survived more thermal cycles than Sn-$BaTiO_3$ [3] for which the Sn matrix is weaker (of strength ~30MPa [4]; 2×10^{-4} strain induces stress ~10MPa). In general, a small or zero spontaneous strain in the inclusions is favorable for achieving the intended response in the composite.

Negative stiffness induced by normal phase transformations is a generic property for ferroelastic materials. For the negative stiffness operated by the defect mechanism, $BaTiO_3$ is not a unique ferroelastic material that possesses such a property. For example, VO_2 [21] exhibited similar OV induced phase transformation like behaviors in the ferroelectric phase (when free of constraint) after ferroelectric aging. Such a defect mechanism induced negative stiffness effect is also expected to be a generic property of ferroelastic materials. In addition, composite properties are not restricted to stiffness and damping; piezoelectricity, thermal expansion, pyroelectricity, and other coupled field properties can be dramatically improved to highly exceed the classical bounds given the presence of a negative stiffness phase. We believe the present work will shed a light on fabricating advanced structural and functional composites with ferroelastic materials as a negative stiffness phase with actuation tunable capability.

To conclude, extreme anelastic composite responses (including stiffness greater than diamond and large amplification of damping) have been achieved in $Zn_{80}Al_{20}$-$BaTiO_3$ composites due to the negative stiffness effect of the $BaTiO_3$ inclusions. Extreme effects can be entailed near the weakly first order (small spontaneous strain) tetragonal-orthorhombic transformation but not the strongly first order (large spontaneous strain) *T*c transformation of $BaTiO_3$, and can be achieved via a defect mechanism in tetragonal $BaTiO_3$ which can be manipulated by specific aging processes.

This work is supported by National Science Foundation.

[1] R.S. Lakes, Physical Review Letter 86 (2001) 2897.
[2]R.S. Lakes, T. Lee, A. Bersie, Y.C. Wang, Nature 410 (2001) 565.
[3]T. Jaglinski, D. Kochmann, D.S. Stone, R.S. Lakes, Science 315 (2007) 620.
[4]T. Jaglinski, R.S. Lakes, Journal of Composite Materials, accepted, March (2011).
[5]W.J. Merz, Physical Review 78 (1950) 52.
[6]X.B. Ren, Nature Materials 3 (2004) 91.
[7]Y. Yang, J. Lan, X. Li, Materials Science and Engineering: A 380 (2004) 378.
[8]T. Lee, R.S. Lakes, A. Lal, Review of Scientific Instruments 71 (2000) 2855.
[9]Arthur S. Nowick, B.S. Berry, Anelastic relaxation in crystalline solids, Academic Press New York and London, 1972.
[10]L. Chen, X.M. Xiong, H. Meng, P. Lv , J.X. Zhang, Applied Physics Letters 89(2006) 0719191.
[11] S.C. Sharma, B.M. Girish, D.R. Somashekar, R. Kamath, B.M. Satish, Composites Science and Technology 59 (1999) 1805.
[12] K.H.W. Seah, S.C. Sharma, M. Krishna, Proceedings Institution of Mechanical Engineers 217 (2003) 201.
[13]K. Yoshimoto, T.S. Jain, K.V. Workum, P.F. Nealey, J.J.de. Pablo, Physical Review Letters 93(2004) 175501.
[14]L. Dong, D.S. Stone, R.S. Lakes, Applied Physics Letters 96 (2010) 141904.
[15]Manufacturer analysis of $BaTiO_3$ (Lot number: I27Q015) shows weight concentrations Al < 0.001%; Mg, Ca, Si < 0.001%; Sr 0.03%, BaO(theory):65.74%; BaO(found):65.41%; TiO_2(theory):34.26%; TiO_2(found):34.25 %. Ti^{3+} (Ti^{4+} can reduce to Ti^{3+}), Al^{3+}, can occupy Ti^{4+} site and form defect polarizations with OV.
[16] C.J.E. Bottcher, Theory of Electric Polarization, Elsevier, Amsterdam, 1952.
[17] W.J. Merz, Physical Review 91(1953) 513.
[18] R.C. Pohanka, R.W. Rice, B.E. Walker, Journal of American Ceramic Society 59 (1976) 71.
[19] R.S. Lakes, W.J. Drugan, Journal of the Mechanics and Physics of Solids 50 (2002) 979.
[20]G. Shirane, A. Takeda, Journal of the Physical Society of Japan 7(1952)1.
[21]X.M. Xiong, L. Chen, L.L. Zhang, X.Y. Wu, C.M. Zheng, J.X. Zhang, Applied Physics Letters 88 (2006)132906.

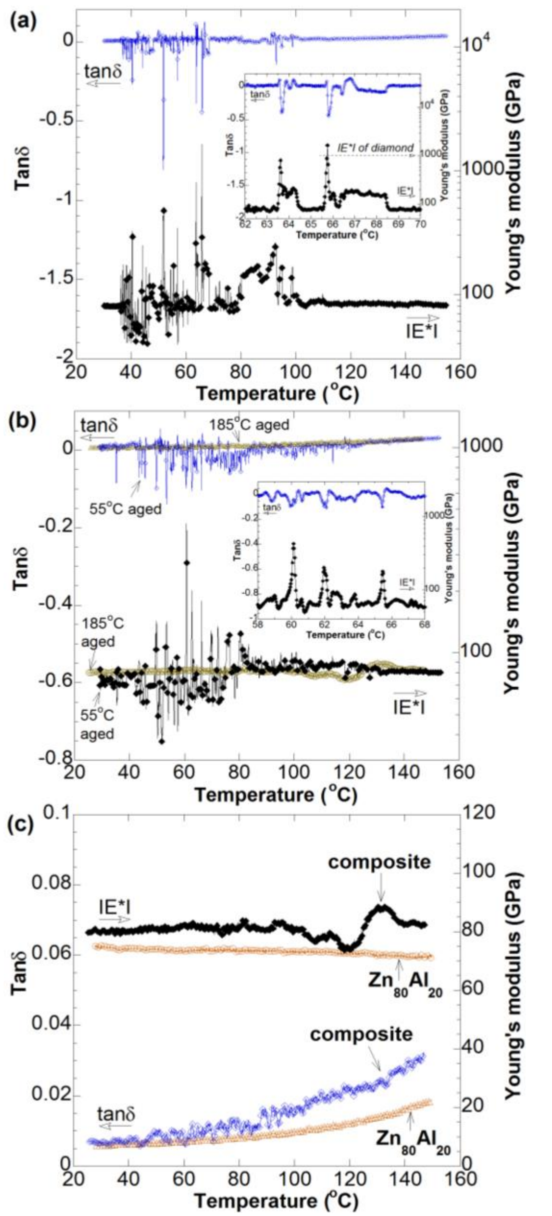

Figure 1. (Color online) Extreme excursions in Young's modulus ($|E^*|$) and damping ($\tan\delta$) of $Zn_{80}Al_{20}$-$BaTiO_3$ composite specimen I at 100Hz. (a) and (b) show results for consecutive heating scans (5% of total data points are shown) after 55°C aging 20h. Insets (100% of data points) show details of anomalies. 185°C aging eliminates the anomalies ((b) and (c)). No anomaly was seen in $Zn_{80}Al_{20}$ or $Zn_{80}Al_{20}$-SiC (c) after 55°C aging 20h.

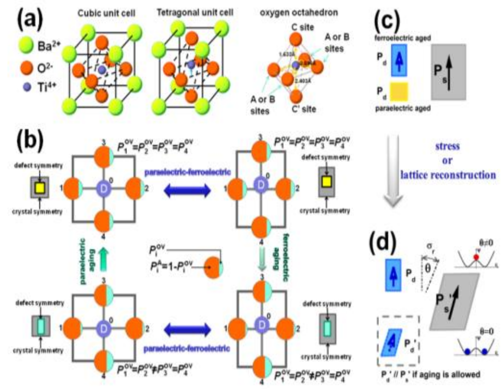

Figure 2. (Color online) (a) $BaTiO_3$ unit cells above and below Tc. The oxygen octahedron in tetragonal $BaTiO_3$ is shown at the right. (b) schematic of crystal symmetries and defect symmetries of $BaTiO_3$ and conditional probabilities of OV occupation at different conditions (adapted from ref. [6]). (c) shows $\mathbf{P_s}$ and $\mathbf{P_d}$ below Tc after "ferroelectric aging" and "paraelectric aging". (d) shows the instantaneous deviation (θ) between $\mathbf{P_s}$ and $\mathbf{P_d}$ under external stress (or lattice reconstruction). Schematic free energy profile within unit cell volumes at the right shows negative stiffness.

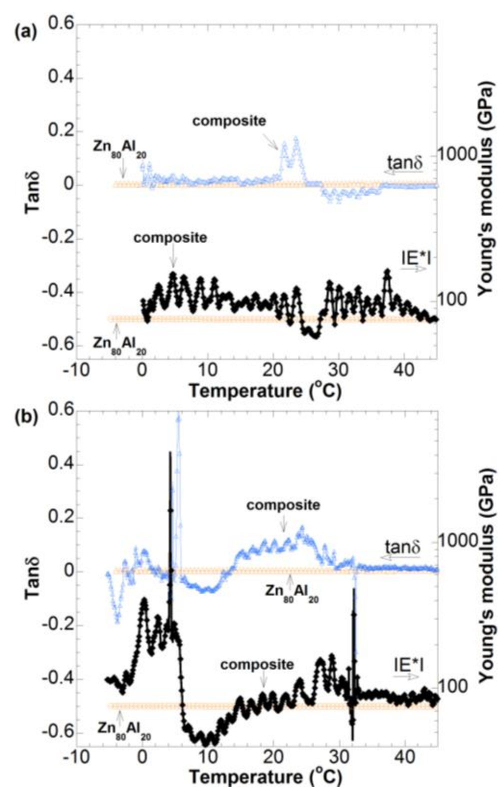

Figure 3. (Color online) Young's modulus ($|E^*|$) and damping ($\tan\delta$) of $Zn_{80}Al_{20}$-$BaTiO_3$ composite specimen II in consecutive heating (a) and cooling (b) scans at 100Hz, showing extreme composite responses near the tetragonal-orthorhombic transformation of $BaTiO_3$ inclusions. No anomaly occurs in $Zn_{80}Al_{20}$ after 75°C aging 18h.